https://doi.org/10.5194/nhess-2020-11
Preprint. Discussion started: 3 February 2020

Natural Hazards and Earth System Sciences
Open Access
EGU
Discussions

Quantitative Risk Assessment of Vehicles Hit by Landslides: A Case Study

Meng Lu[1], Jie Zhang[2*], Lulu Zhang[3] and Limin Zhang[4]

Abstract: Landslides threaten the safety of vehicles on highways. Nevertheless, a rigorous quantitative highway landslide risk assessment seems difficult. Using a case study in Hong Kong, this paper presents a method for quantitative risk assessment for highway landslides. The suggested method consists of three parts, i.e., analysis of annual failure probability of the slope, the spatial impact analysis and the consequence analysis. In the case study, the annual failure probability of the slope is analyzed based on historical failure data in Hong Kong. The spatial impact of the landslides is estimated based on empirical correlations with the geometry of the slope. The consequence is assessed based on probabilistic modeling of the traffic on the highway. Based on the suggested method, the annual failure probability of the slope, the distance from the slope and the road and the density of vehicles on the road can significantly affect the landslide risk and the suggested method can be used to quantify the effects of these factors. The suggested method can be also potentially used to analyze the highway landslide risk in other regions.

Key words: Landslides; Vehicles; Risk assessment; Historical failure data; Probabilistic modeling

[1] Research Assistant, Key Laboratory of Geotechnical and Underground Engineering of Ministry of Education and Department of Geotechnical Engineering, Tongji University, Shanghai 200092, China. E-mail: lumeng@tongji.edu.cn
[2] Professor, Key Laboratory of Geotechnical and Underground Engineering of Ministry of Education and Department of Geotechnical Engineering, Tongji University, Shanghai 200092, China. E-mail: cezhangjie@tongji.edu.cn
[3] Professor, State Key Laboratory of Ocean Engineering and Department of Civil Engineering, Shanghai Jiao Tong University, Shanghai 200240, China. E-mail: lulu_zhang@sjtu.edu.cn
[4] Professor, Department of Civil Engineering, Hong Kong University of Science and Technology, Clear Water Bay, Hong Kong, China. E-mail: cezhangl@ust.hk

https://doi.org/10.5194/nhess-2020-11
Preprint. Discussion started: 3 February 2020

Natural Hazards and Earth System Sciences
Discussions

1 Introduction

With a total land area of about 1100 km^2, Hong Kong is one of the most densely populated regions in the world with a population of about 7.5 million (GovHK, 2019). Throughout the territory of Hong Kong, there are more than 57, 000 registered man-made slope features (Cheung and Tang, 2005). With an average annual rainfall of about 2400 mm, rainfall induced landslides are one of the major natural hazards threatening the public safety in Hong Kong (GEO, 2017). In particular, slope failures along highways have resulted in serious fatalities, damaged vehicles and disruption to the traffic. For example, in August 1994, a public light bus on the Castle Peak Road was hit by landslide debris, causing three persons trapped inside the bus and one man killed. In August 1995, the slope along Shum Wan Road failed, induced by large rainfall, which resulted in two fatalities and five injuries. In August 1997, the landslide along Ching Cheung Road resulted in the closure of the highway for more than three weeks (GEO, 2017). Similar phenomena have indeed also been reported in many other parts of the world (Bil et al., 2015), such as Italy (Donnini et al., 2017) and India (Negi et al., 2013).

There are many uncertainties in the assessment of the hazard of moving vehicles hit by landslides, such as the occurrence of landslides, the travel distance of the landslide and the presence of the moving vehicles at the moment of landslides. Risk assessment is a framework in which both the uncertainties and the consequence of a hazard can be addressed, which is now increasingly been used for landslide risk management (e.g. Lessing et al., 1983; Fell, 1994; Dai et al., 2002; Remondo et al., 2008; Erener, 2012; Vega and Hidalgo, 2016). Indeed, landslide risk assessment has been accepted as an effective tool for the planning of land use in Hong Kong. Nevertheless, the risk assessment of moving vehicles attacked by landslides is special in that the elements at risk are highly mobile. Several studies have also been conducted on assessing the impact probability of landslides

https://doi.org/10.5194/nhess-2020-11
Preprint. Discussion started: 3 February 2020

Natural Hazards and Earth System Sciences
Open Access
EGU
Discussions

on vehicles (e.g. Budetta, 2004; Peila and Guardini, 2008; Nicolet et al., 2016). Fell et al. (2005) assessed the probability of a falling block hitting a vehicle based on the length of the vehicle and the traffic flow. Dorren et al. (2009) suggested a method to assess the probability of a vehicle hit by a landslide based on the dimension of the landslide and the traffic flow. Michoud et al. (2012) assessed the probability of a vehicle hit by a falling rock considering the dimensions of the vehicle and size of falling rocks. However, few attempts have been made to suggest a rigorous assessment framework of vehicles hit by landslides. As such, implementation of rigorous risk assessment of vehicles hit by landslides is still challenging.

Through a case study in Hong Kong, the objective of this paper is to suggest a method to quantitatively assess the risk of vehicles hit by landslides along highways. The structure of this paper is as follows. Firstly, how the annual failure probability of the slope is calculated is described. Then, the spatial impact of the landslide is analyzed. Thereafter, the consequence of the landslide is analyzed. Finally, the annual risk of vehicles hit by the landslide is calculated. The assessment method provides a convenient and useful tool to investigate the risk of vehicles hit by landslides in Hong Kong.

2 Engineering Background

Fig. 1 shows the slope under investigation in this study, which is along the Kennedy Road in the Wan Chai district of Hong Kong. Wan Chai is one of the oldest and most traditional cultural areas in Hong Kong and attracts many tourists. According to Transport Department of Hong Kong (TDHK) (2018), Kennedy Road is a major road with three lanes in this region. Fig. 2 shows a typical cross section of the slope. The height of the slope, *H*, is 26 m and the slope angle is about 45 degrees. As shown in

https://doi.org/10.5194/nhess-2020-11
Preprint. Discussion started: 3 February 2020

Natural Hazards and Earth System Sciences
Discussions

this figure, the horizontal distance from the crest of the landslide scar to the side of Kennedy Road close to the slope, l_{ch}, is about 35 m and the horizontal distance from the slope toe to the side of Kennedy Road close to the slope, l_{th}, is about 3 m. The width of Kennedy Road, b_h, is 10 m. Fig. 3 shows the plan view of the slope. The landslide scar is about 25 m in length and about 18 m in width. On 8 May 1992, the slope failed during an intense rainfall, which hit a car travelling along Kennedy Road and killed the driver (GEO, 1996). According to TDHK (2018), vehicles in Hong Kong are composed of private buses, non-franchised public buses, franchised buses, taxis, private cars, public light buses, private light buses, goods vehicles, special purpose vehicles, government vehicles and motor cycles. The percentage of each type of vehicle with respect to total numbers of vehicles is shown in Table 1 (TDHK, 2018). According to TDHK (2018), the typical length of each type of vehicle is also shown in Table 1. The purpose of this case study is to analyze the risk of vehicles hit by the landslide if this slope fails again.

3 Methodology

In general, the risk of a landslide hazard depends on the likelihood of the landslide, the spatial extent of the landslide and the number of vehicles being hit by the landslide. There are multiple types of vehicles on a highway. The longer the vehicle, the greater the probability that it will be hit by a landslide. Let $P(F)$ denote the annual probability of slope failure. Suppose there are m possible spatial impacts and let $P(\mathbf{S} = \mathbf{S}_i| F)$ denote the chance that the spatial impact is $\mathbf{S}_i$ when the landslide occurs. Let $P(n_j = k| \mathbf{S} = \mathbf{S}_i)$ denote the chance that the k type j vehicle will be hit by the landslide when the spatial impact is $\mathbf{S}_i$. The risk associated with the jth type of vehicle, i.e., the expected annual number of type j vehicles being hit by the landslide, can be calculated as follows:

https://doi.org/10.5194/nhess-2020-11
Preprint. Discussion started: 3 February 2020

$$R_{vj} = P(F) \times \sum_{i=1}^{m} \left[P(\mathbf{S} = \mathbf{S}_i \mid F) \times \sum_{k=1}^{\infty} kP(n_j = k \mid \mathbf{S} = \mathbf{S}_i) \right] \tag{1}$$

Let n_v denote total types of vehicles. The total risk of vehicles hit by the landslide considering all types of vehicles, i.e., R_v, can then be calculated as follows:

$$R_v = \sum_{j=1}^{n_v} R_{vj} \tag{2}$$

Let n_{pj} denote the average number of persons in a type j vehicle. The risk of people hit by the landslide can be calculated as follows:

$$R_{pj} = P(F) \times \sum_{i=1}^{m} \left[P(\mathbf{S} = \mathbf{S}_i \mid F) \times \sum_{k=1}^{\infty} kP(n_j = k \mid \mathbf{S} = \mathbf{S}_i) \right] \times n_{pj} \tag{3}$$

The total risk of people hit by the landslide considering all types of vehicles can be calculated as follows:

$$R_p = \sum_{j=1}^{n_v} R_{pj} \tag{4}$$

As can be seen from the above equations, the keys for risk assessment are to evaluate: (1) the annual failure probability of the landslide, i.e., $P(F)$, (2) the spatial impact of the landslide, i.e., $P(\mathbf{S} = \mathbf{S}_i | F)$ and (3) the number of vehicles being hit by the landslide for a given spatial extent, i.e., $P(n_j = k | \mathbf{S} = \mathbf{S}_i)$. How the above elements are assessed is introduced in the following sections.

3.1 Evaluation of annual probability of the landslide, $P(F)$

The estimation of the probability of occurrence of landslides within a given period of time is fundamental in landslide hazard assessment. Since almost slope failures in Hong Kong are caused by rainfall infiltration (e.g. Lumb, 1975; Brand, 1984; Finlay et al., 1999), assessing annual probability of rainfall-induced landslides is important. In general, there are two types of methods for evaluating

https://doi.org/10.5194/nhess-2020-11
Preprint. Discussion started: 3 February 2020

the likelihood of slope failure within a given exposure time: methods through slope stability analysis built on principles of soil mechanics (e.g. Christian et al., 1994; Fenton and Griffiths, 2005; Huang et al., 2010) and empirical methods through statistical analysis of historical slope failure data (e.g. Chau et al., 2004; Tang and Zhang, 2009). Currently, landslide probability analyses via slope stability analyses mainly focus on the likelihood of slope failure for a given rainfall. As an illustration, the statistical methods are used to estimate the annual landslide probability.

In Hong Kong, the failure of a slope is highly correlated to the 24-hour rainfall, i_{24} (Cheung and Tang, 2005). Zhang and Tang (2009) divided the rainfall events in Hong Kong into three categories based on i_{24}, i.e., (1) i_{24} < 200 mm/day (small rainfall, denoted as *SR*), (2) 200 mm < i_{24} < 400 mm/day (medium rainfall, denoted as *MR*) and (3) i_{24} > 400 mm/day (large rainfall, denoted as *LR*). Based on slope failure data observed in Hong Kong during 1984-2002, it is found that the failure probability of an average slope in Hong Kong when subjected to small rainfall, medium rainfall and large rainfall is 1.09×10^{-4}, 2.61×10^{-3} and 8.94×10^{-3} , respectively (Zhang and Tang, 2009), i.e., $P(F| SR) = 1.09 \times 10^{-4}$, $P(F| MR) = 2.61 \times 10^{-3}$ and $P(F| LR) = 8.94 \times 10^{-3}$. The above analyses provide the conditional failure probability of a slope for a given type of rainfall. To evaluate the annual probability of slope failure, the probability of each type of rainfall should be analyzed. For such a purpose, Fig. 4 shows the histogram of the yearly maximum i_{24} measured at Hong Kong Observatory Headquarters during 1969 and 2018 (HKO, 2018). As can be seen from Fig. 4, the maximum i_{24} in a year in Hong Kong is mainly in the range of 100 to 350 mm. The generalized extreme value distribution (Hosking et al., 1985) with the following probability density function (PDF) seems to fit the histogram with reasonable accuracy:

https://doi.org/10.5194/nhess-2020-11
Preprint. Discussion started: 3 February 2020

Natural Hazards and Earth System Sciences
Discussions

$$f\left(i_{24}\right) = \frac{1}{\beta}\left[1 + \gamma\left(\frac{i_{24} - \mu}{\beta}\right)\right]^{-\frac{1}{\gamma}} \exp\left\{\left[1 + \gamma\left(\frac{i_{24} - \mu}{\beta}\right)\right]^{-\frac{1}{\gamma}}\right\} \tag{5}$$

where β, μ and γ are the scale parameter, the location parameter and the shape parameter of the generalized extreme distribution, respectively. The values of β, μ and γ can be calculated based on maximum likelihood method and they are equal to -0.17, 66 and 188, respectively. Fig. 5 shows the cumulative distribution function (CDF) of i_{24} obtained based on the fitted generalized extreme value distribution. As can be seen from this figure, the probability that the rainfall with yearly maximum i_{24} belongs to small rainfall, medium rainfall and large rainfall is 0.44, 0.55 and 0.01, respectively, i.e., $P(SR) = 0.44$, $P(MR) = 0.55$ and $P(LR) = 0.01$. Based on the total probability theorem, the annual probability of slope failure can be computed as follows:

$$P\left(F\right) = P\left(F \mid SR\right) P\left(SR\right) + P\left(F \mid MR\right) P\left(MR\right) + P\left(F \mid LR\right) P\left(LR\right) \tag{6}$$

3.2 Evaluation of spatial impact of the landslide, $P(\mathbf{S} = \mathbf{S}_i | F)$

The spatial impact of a landslide depends on whether the landslide can reach the highway and the length of the affected road if the landslide can reach the highway. In general, methods to investigate the travel distance of a landslide can be divided into two categories (Hungr et al., 2005), i.e., (1) analytical or numerical methods based on the physical laws of solid and fluid dynamics (Scheidegger, 1973), which are often solved numerically (e.g. Hungr and McDougall, 2009; Luo et al., 2019) and (2) empirical methods based on field observations (e.g. Budetta and Riso, 2004; Dai and Lee, 2002). Since the empirical method is more convenient to apply (Finlay et al., 1999), it is used in this paper. As illustrated in Fig. 2, the travel distance of the sliding mass (L) is highly related to the volume (V) and height (H) of sliding body (e.g. Corominas, 1996; Liang et al., 2017). According to historical

https://doi.org/10.5194/nhess-2020-11
Preprint. Discussion started: 3 February 2020

data in Hong Kong, Corominas (1996) found that the travel distance of landslide debris can be estimated using the following equation:

$$\log L = 0.085\log V + \log H + 0.047 + \varepsilon \tag{7}$$

where ε is a random variable with a mean of zero and a standard deviation of $\sigma = 0.161$.

For the slope as shown in Fig. 2, the height is 25 m, i.e., H = 25 m. To apply Eq. (7), the landslide volume is needed. Let A_s denote the landslide scar area, which can be related to landslide volume through empirical relationships (e.g. Malamud et al., 2004; Imaizumi and Sidle, 2007; Guzzetti et al., 2008; Guzzetti et al., 2009). In this study, the power relationship suggested by Parker (2011) is used:

$$V = 0.106 \times A_s^{1.388} \tag{8}$$

Based on Fig. 3, the landslide scar area is estimated to be 450 m^2. Based on Eq. (8), the volume is estimated about 510 m^3, which is close to the real volume of sliding mass in the landside event on 8 May 1992 (GEO, 1996). Substituting the values of H and V into Eq. (7), it can be obtained that the travel distance of the landslide is lognormally distributed with a mean of 50.7 m and a standard deviation of 12.6 m. Fig. 6 shows the PDF of the travel distance of the landslide. As can be seen from this figure, the value of travel distance of the landslide is mainly in the range of 20 m to 150 m.

The spatial extent of the landslide is also related to the length of the affected road. As shown in Fig. 3, when the head or the rear of a vehicle contacts with the landslide mass, the vehicle will be hit by the landslide, i.e., the number of vehicles being hit by landslides depends on the width of the landslide (b_l) and the length of the vehicles (l_v). The length of affected road, l_a, is the sum of the width of the landslide and the length of vehicles, i.e.,

$$l_a = b_l + 2l_v \tag{9}$$

In this study, the spatial extent of the landslide is characterized by the length of the affected road and the runout distance of the landslide, i.e., $\mathbf{S} = \{l_a, L\}$. For simplicity, the uncertainty associated with the length of the affected road is not considered. In such a case, the uncertainty associated with $\mathbf{S}$ is fully characterized by the uncertainty associated with the runout distance. In principle, the runout distance is a continuous random variable. For simplicity, it can be discretized into a discrete variable. Let L_i denote the ith possible value of L and let $\mathbf{S}_i = \{l_a, L_i\}$. $P(\mathbf{S} = \mathbf{S}_i | F)$ can be calculated by

$$P\left(\mathbf{S} = \mathbf{S}_i \mid F\right) = P\left(L = L_i\right) \tag{10}$$

3.3 Evaluation of encounter probability, $P(n_j = k | \mathbf{S} = \mathbf{S}_i)$

As shown in Fig. 2, the horizontal distance from the crest of the landslide scar to the side of Kennedy Road close to the slope is about 35 m, i.e., l_{ch} = 35 m. The width of Kennedy Road is about 10 m, i.e., b_h = 10 m. The landslide will reach Kennedy Road once $L > l_{ch}$. When $L \geq l_{ch} + b_h$, the Kennedy Road will be totally covered by the sliding mass. When $l_{ch} < L < l_{ch} + b_h$, the Kennedy Road will be partially affected. Thus, the proportion of vehicles within the affected length of the Kennedy Road which will be hit by the landslide, denoted as $\alpha(\mathbf{S} = \mathbf{S}_i)$ here, can be calculated as follows:

$$\alpha\left(\mathbf{S} = \mathbf{S}_i\right) = \begin{cases} 0, & L_i \leq l_{ch} \\ \dfrac{L_i - l_{ch}}{b_h}, & l_{ch} < L_i < l_{ch} + b_h \\ 1, & L_i \geq l_{ch} \end{cases} \tag{11}$$

In general, the number of vehicles hit by landslides highly depends on the density of vehicles, the spatial extent of the landslide and the size of the vehicles. The presence of the vehicles on a highway can be modeled as a Poisson process with a mean arrival rate of λ (Paxson and Floyd, 1995). Let q denote the number of vehicles passing a given cross section of a road per unit time. Let v

https://doi.org/10.5194/nhess-2020-11
Preprint. Discussion started: 3 February 2020

Natural Hazards and Earth System Sciences
Open Access
Discussions

denote the average speed of the vehicles. The mean rate of occurrence of moving vehicles, λ, can be calculated as follows (Lighthill, 1995):

$$\lambda = \frac{q}{v} \tag{12}$$

Let w_j denote the proportion of type j vehicle in the traffic flow. The mean rate of occurrence of type j vehicle can be then written as follows:

$$\lambda_j = w_j \times \frac{q}{v} \tag{13}$$

As an example, Table 2 shows the data about q and v of the Kennedy road for the morning peak, normal period and evening peak, respectively, which are obtained from TDHK (2018). As shown in Fig. 3, the width of the landslide is about 18 m, i.e., $b_l = 18$ m. The length of each type of vehicle, l_v, are shown in Table 1. Based on these data, the mean rate of occurrence of each type of vehicle can be calculated for different periods of a day, as shown in Figs. 7(a)–(c), respectively. It can be seen that the mean rate of occurrence of the vehicles during the morning and evening peak is significantly larger than that in the normal period. Among all types of vehicles, the mean rate of private cars in the affected road is the greatest, followed by goods vehicles, motor cycles and taxis.

Let T_1, T_2 and T_3 denote the morning peak, the normal period and the evening peak, respectively; and l_{aj} denote the length of affected road for type j vehicle. Based on the property of a Poisson process, if the spatial impact is $\mathbf{S} = \mathbf{S}_i$ and the slope fails during period T_i, the chance that k type j vehicles will be hit by the landslide can be computed by

$$P\left(n_j = k \mid t \in T_i, \mathbf{S} = \mathbf{S}_i\right) = \frac{\left[\alpha_j\left(\mathbf{S} = \mathbf{S}_i\right)\lambda_j l_{aj}\right]^k}{k\,!} \exp\left[-\alpha_j\left(\mathbf{S} = \mathbf{S}_i\right)\lambda_j l_{aj}\right] \tag{14}$$

As an example, Figs. 8(a)–(c) shows the distributions of the number of private cars hit by the landslide for the case of $\alpha_j(\mathbf{S} = \mathbf{S}_i) = 1$ when the slope failure occurs during the morning peak, normal

https://doi.org/10.5194/nhess-2020-11
Preprint. Discussion started: 3 February 2020

period and evening peak, respectively. As can be seen from these figures, the most probable number of private cars hit by the landslide when the slope failure occurs during the morning peak and evening peak is both about 3 and its probability is both about 0.20. The most probable number of private cars hit by the landslide when the slope failure occurs during the normal period is about 1 and its probability is about 0.37.

In Eq. (14), the failure time is assumed known. In reality, the slope can fail during any period of a day. Based on the total probability theorem, the probability that k Type j vehicles will be hit for the case of $\mathbf{S} = \mathbf{S}_i$ can be computed by

$$P\left(n_j = k \mid \mathbf{S} = \mathbf{S}_i\right) = \sum_{i=1}^{3} P\left(n_j = k \mid t \in T_i, \mathbf{S} = \mathbf{S}_i\right) P\left(t \in T_i\right) \tag{15}$$

As an example, Figs. 8(d) shows the probability distribution of the number of private cars hit by the landslide for $\alpha_j(\mathbf{S} = \mathbf{S}_i) = 1$ considering the uncertainty of the failure time. As can be seen from this figure, the most probable number of private cars hit by the landslide considering the uncertainty of the failure time is about 1 and its probability is about 0.32.

3.4 Risk assessment

In the above analyses, equations for evaluating $P(F)$, $P(\mathbf{S} = \mathbf{S}_i \mid F)$ and $P(n_j = k \mid \mathbf{S} = \mathbf{S}_i)$ are introduced. Substituting these equations into Eq. (1), the risk of each type of vehicles hit by the landslide studied in this paper can then be calculated, which are shown in Figs. 9(a). As can be seen from this figure, the annual risk of private cars hit by the landslide is the greatest with a value of 1.67×10^{-3} vehicles per year, followed by the goods vehicles, motor cycles and taxis. The risk associated with each type of vehicle is highly correlated with the proportion of vehicles in the traffic flow. The private cars have the greatest proportion in the traffic flow and hence it is natural to be associated with the

https://doi.org/10.5194/nhess-2020-11
Preprint. Discussion started: 3 February 2020

greatest risk. In reality, the vehicle that was hit by the studied slope on 8 May 1992 was indeed a private car. With Eq. (2), the risk of vehicles hit by the landslide considering all types of vehicles can be also calculated, which is about 2.48×10^{-3} vehicles per year.

The passenger capacity of each type of vehicle can be investigated through TDHK (2018) and the assumed average number of persons in a vehicle is also shown in Table 1. Submitting these numbers into Eq. (3), the risk of persons hit by the landslide associated with each type of vehicle can be computed and the results are shown in Figs. 9(b). As can be seen from this figure, the annual risk of persons hit by the landslide for private cars is the greatest with a value of 8.37×10^{-3} persons per year, followed by non-franchised public buses, franchised buses and goods vehicles. The risk to persons for each type of vehicles highly depends on the proportion of vehicles in the traffic flow and the passenger capacity of vehicles. The non-franchised public buses have the higher proportion in the traffic flow and the largest passenger capacity hence it is natural to be associated with the greater risk. Based on Eq. (4), the risk of persons hit by the individual landslide studied in this paper considering all types of vehicles can be also calculated, which is about 1.36×10^{-2} persons per year.

4 Discussions

4.1 Effect of annual failure probability of the slope

In the above analysis, the annual failure probability of the slope is 1.58×10^{-3}, which is calculated based on historical data in Hong Kong and represents the failure probability of an average slope in Hong Kong. To investigate the effect of the failure probability of the slope, Fig. 10 shows the annual risk of the slope calculated based on different annual failure probabilities. As can be seen from this figure, the annual risk to all types of vehicles increases linearly with the annual failure probability of

https://doi.org/10.5194/nhess-2020-11
Preprint. Discussion started: 3 February 2020

the slope. When the failure probability of the slope increase from 1.0×10^{-4} to 1.0×10^{-2}, the annual risk to vehicles increases from 1.57×10^{-4} vehicles being hit per year to 1.57×10^{-2} vehicles being hit per year. A similar observation can also be found for the annual risk to persons. Hence, reducing the annual failure probability of a slope is an effective means to reduce the risk of the slope.

4.2 Effect of distance from the slope to the highway

The risk of damaged vehicles due to landslides is highly associated with spatial impact of landslides. The further the road is away from the slope, the less chance the road will be affected by the slope. In the above analysis, the horizontal distance from the crest of the landslide scar to the side of Kennedy Road close to the slope, l_{ch}, is about 35 m and the horizontal distance from the slope toe to the side of Kennedy Road close to the slope, l_{th}, is about 3 m (GEO, 1996). To study the effect of the distance from the road to the slope, the annual risk to different types of vehicles and persons along Kennedy Road are calculated as the distance between the slope and the road varies, and the results are shown in Figure 11. As can be seen from this figure, the annual risk to vehicles along Kennedy Road is reduced as l_{th} becomes larger. When l_{th} / H = 0.7, the risk is reduced by half compared the case of l_{th} / H = 0.1. When l_{th} / H is 2, the risk is negligible. Thus, increasing the distance between the slope and the road can effectively reduce the risk of landslides.

4.3 Effect of traffic flow

As can be seen from Fig. 7, since the number of vehicles during different periods in a day is different, the mean rate of occurrence of vehicles in affected road due to the landslide is significantly different. The high density of vehicles may pose a huge risk to vehicles and persons due to landslides. To indicate the effect of density of vehicles on the landslide risk, the annual risk to all types of vehicles and persons along Kennedy Road are investigated when the density of vehicles on the highway increases from 0 to 300 vehicles per kilometer and the results are shown in Fig. 12. As can be seen from this figure, there is a linear increasing trend of the annual risk to all types of vehicles and persons as density of vehicles increases. When the density of vehicles is equal to 300 vehicles per kilometer, the annual risk to vehicles and persons can reach 1.01×10^{-2} vehicles being hit per year and 5.52×10^{-2} persons being hit per year, respectively. Therefore, the high density of vehicles will significantly enhance the annual risk to vehicles and persons due to landslides and properly managing transportation and ensuring smooth traffic flow are important to reduce the risk.

5 Summary and Conclusions

Quantitative assessment the risk of vehicles hit by landslides can help better understand and manage such kind of risk. Using a case study in Hong Kong, this paper suggests a method to assess the risk of highway landslide. For the slope studied in this paper, the annual failure probability is first assessed based on historical slope failure data in Hong Kong. The spatial impact of the landslide is then analyzed using an empirical round out analysis method. The consequence of the landslide is assessed by modeling the traffic on the highway as a Poisson process. For the slope examined in this paper, it is found that different types of vehicles may be associated with different levels of risk. Also, it is found that the annual failure probability of the slope, the distance from the slope and the road and the density of vehicles on the road can significantly affect the landslide risk and the suggested method can be used to quantify the effect of the above factors. The suggested method can also be potentially used to analyze the highway landslide risk in other regions.

Acknowledgements

This research was substantially supported by the National Key Research and Development Program of China (2018YFC0809600, 2018YFC0809601), the National Natural Science Foundation of China (41672276，51538009), the Key Innovation Team Program of MOST of China (2016RA4059), and Fundamental Research Funds for the Central Universities.

References

Bíl, M., Vodák, R., Kubeček, J., Bílová, M., and Sedoník, J.: Evaluating road network damage caused by natural disasters in the czech republic between 1997 and 2010, Transportation Research Part A, 80, 90–103, 2015.

Budetta, P., and Riso, R. D.: The mobility of some debris flows in pyroclastic deposits of the northwestern Campanian region (southern Italy), Bulletin of Engineering Geology and the Environment, 63, 293–302, 2004.

Brand, E.W.: Landslides in Southeast Asia: A State-of-the-art Report, in: Proceedings of the 4th International Symposium on Landslides, Toronto, Vol. 1, pp. 17–59, 1984.

Budetta, P.: Assessment of rockfall risk along roads, Natural Hazards and Earth System Sciences, 4, 71-81, 2004.

Christian, J. T., Ladd, C. C., and Baecher, G. B.: Reliability applied to slope stability analysis, Journal of Geotechnical Engineering, ASCE, 120, 2180–2207, 1994.

Chau, K. T., Sze, Y. L., Fung, M. K., Wong, W. Y., Fong, E. L., and Chan, L. C. P.: Landslide hazard analysis for Hong Kong using landslide inventory and GIS, Computers and Geosciences, 30, 429–443, 2004.

https://doi.org/10.5194/nhess-2020-11
Preprint. Discussion started: 3 February 2020

Cheung, R. W. M., and Tang, W. H.: Realistic assessment of slope reliability for effective landslide hazard management, Geotechnique, 55, 85–94, 2005.

Corominas, J.: The angle of reach as a mobility index for small and large landslides, Canadian Geotechnical Journal, 33, 260–271, 1996.

Donnini, M., Napolitano, E., Salvati, P., Ardizzone, F., Bucci, F., and Fiorucci, F., et al.: Impact of event landslides on road networks: a statistical analysis of two Italian case studies, Landslides, 14, 1–15, 2017.

Dai, F. C., Lee, C. F., and Ngai, Y. Y.: Landslide risk assessment and management: an overview, Engineering Geology, 64, 65–87, 2002.

Dorren, L., Sandri, A., Raetzo, H., and Arnold, P.: Landslide risk mapping for the entire Swiss national road network, in: Malet, J. P., Remaître, A., and Bogaard, T. (Eds.), Landslide Processes: From Geomorphologic Mapping to Dynamic Modelling, Utrecht University and University of Strasbourg, Strasbourg, pp. 6–7, 2009.

Dai, F., and Lee, C.: Landslide characteristics and slope instability modeling using GIS, Lantau Island, Hong Kong, Geomorphology, 42, 213–228, 2002.

Erener, A.: A regional scale quantitative risk assessment for landslides: Case of kumluca watershed in Bartin, Turkey, Landslides, 10, 55–73, 2012.

Fenton, G. A., and Griffiths, D. V.: A slope stability reliability model, in: Proceeding of the K.Y. Lo Symposium (on CD), London, Ontario, 2005.

Finlay, P. J., Mostyn, G. R., and Fell, R.: Landslide risk assessment: prediction of travel distance, Canadian Geotechnical Journal, 36, 556–562, 1999.

Fell, R., Ho, K. K. S., Lacasse, S., and Leroi, E.: A framework for landslide risk assessment and management, in: Hungr, O., Fell, R., Couture, R., and Eberhardt, E. (Eds.), Landslide Risk Management, Taylor and Francis, London, pp. 3–26, 2005.

Fell, R.: Landslide risk assessment and acceptable risk, Canadian Geotechnical Journal, 31, 261–272, 1994.

GovHK: Hong Kong–the Facts, Retrieved from www.gov.hk, 2019.

Gao, L., Zhang, L. M., and Chen, H. X.: Likely scenarios of natural terrain shallow slope failures on Hong Kong Island under extreme storms, Natural Hazards Review, 18, B4015001, 2017.

GEO (Geotechnical Engineering Office): Highway slope manual, Civil Engineering and Development Dept., Government of Hong Kong SAR, Hong Kong, 2017.

GEO (Geotechnical Engineering Office): Investigation of some major slope failures between 1992 and 1995, Civil Engineering and Development Dept., Government of Hong Kong SAR, Hong Kong, 1996.

Guzzetti, F., Ardizzone, F., Cardinali, M., Galli, M., Reichenbach, P., and Rossi, M.: Distribution of landslides in the Upper Tiber River basin, central Italy, Geomorphology, 96, 105−122, 2008.

Guzzetti, F., Ardizzone, F., Cardinali, M., Rossi, M., and Valigi, D.: Landslide volumes and landslide mobilization rates in Umbria, central Italy, Earth and Planetary Science Letters, 279, 0–229, 2009.

Huang, J., Griffiths, D. V., and Fenton, G. A.: System reliability of slopes by RFEM, Soils and Foundations, 50, 343−353, 2010.

Hosking, J. R. M., Wallis, J. R., and Wood, E. F.: Estimation of the generalized extreme-value distribution by the method of probability-weighted moments, Technometrics, 27, 251–261, 1985.

Hungr, O., and McDougall, S.: Two numerical models for landslide dynamic analysis, Computers and Geosciences, 35, 978–992, 2009.

Hungr, O., Corominas, J., and Eberhardt, E.: Estimating landslide motion mechanism, travel distance and velocity, in: Hungr, O., Fell, R., Couture, R., and Eberhardt, E. (Eds.), Landslide Risk Management, Taylor and Francis, London, pp. 99−128, 2005.

HKO (Hong Kong Observatory): Climate Statistics, Retrieved from www.hko.gov.hk, 2018.

https://doi.org/10.5194/nhess-2020-11
Preprint. Discussion started: 3 February 2020

Natural Hazards and Earth System Sciences
Open Access
Discussions

Imaizumi, F., and Sidle, R. C.: Linkage of sediment supply and transport processes in Miyagawa Dam catchment, Japan, Journal Geophysical Research, 112, F03012, 2007.

Lessing, P., Messina, C. P., and Fonner, R. F.: Landslide risk assessment. Environmental Geology, 5, 93–99, 1983.

Luo, H. Y., Zhang, L. L., and Zhang, L. M.: Progressive failure of buildings under landslide impact, Landslides, 16, 1327–1340, 2019.

Lighthill, M., J.: On kinematic waves ii. a theory of traffic flow on long crowded roads, Proceedings of the Royal Society, A Mathematical Physical & Engineering Sciences, 229, 317–345, 1955.

Lumb, P.: Slope failures in Hong Kong. Quarterly Journal of Geology, 8, 31–65, 1975.

Michoud, C., Derron, M. H., Horton, P., Jaboyedoff, M., Baillifard, F. J., Loye, A., Nicolet, P., Pedrazzini, A., and Queyrel, A.: Rockfall hazard and risk assessments along roads at a regional scale: example in Swiss Alps, Natural Hazards and Earth System Sciences, 12, 615–629, 2012.

Malamud, B. D., Turcotte, D. L., Guzzetti, F., and Reichenbach, P.: Landslide inventories and their statistical properties. Earth Surface Processes and Landforms, 29, 687–711, 2004.

Nicolet, P., Jaboyedoff, M., Cloutier, C., Crosta, G. B., and Lévy, S.: Brief communication: on direct impact probability of landslides on vehicles, Natural Hazards and Earth System Sciences, 16, 995–1004, 2016.

Negi, I. S., Kumar, K., Kathait, A., and Prasad, P. S.: Cost assessment of losses due to recent reactivation of Kaliasaur landslide on National Highway 58 in Garhwal Himalaya, Natural Hazards, 68, 901–914, 2013.

Paxson, V., and Floyd, S.: Wide-area traffic: The failure of Poisson modeling, IEEE/ACM Transactions on Networking, 3, 226–244, 1995.

Parker, R. N., Densmore, A. L., Rosser, N. J., De Michele, M., Li, Y., and Huang, R., et al.: Mass wasting triggered by the 2008 Wenchuan earthquake is greater than orogenic growth, Nature Geoscience, 4, 449–452, 2011.

https://doi.org/10.5194/nhess-2020-11
Preprint. Discussion started: 3 February 2020

Natural Hazards and Earth System Sciences
Discussions

Peila, D., and Guardini, C.: Use of the event tree to assess the risk reduction obtained from rockfall protection devices, Natural Hazards and Earth System Sciences, 8, 1441–1450, 2008.

Remondo, J., Bonachea, J., and Cendrero, A.: Quantitative landslide risk assessment and mapping on the basis of recent occurrences, Geomorphology, 94, 496–507, 2008.

Scheidegger, A. E.: On the prediction of the reach and velocity of catastrophic landslides, Rock Mechanics and Rock Engineering, 5, 231–236, 1973.

Transport Department of Hong Kong (TDHK): Transport in Hong Kong, Retrieved from www.td.gov.hk, 2018.

Vega, J. A., and Hidalgo, C. A.: Quantitative risk assessment of landslides triggered by earthquakes and rainfall based on direct costs of urban buildings, Geomorphology, 273, 217–235, 2016.

Zhang, J., and Tang, W. H.: Study of time-dependent reliability of old man-made slopes considering model uncertainty, Georisk: Assessment and Management of Risk for Engineered Systems and Geohazards, 3, 106–113, 2009.

https://doi.org/10.5194/nhess-2020-11
Preprint. Discussion started: 3 February 2020

Natural Hazards and Earth System Sciences Discussions

List of Tables

Table 1. Percent, length and passenger capacity of vehicles in Hong Kong

Table 2. Number of vehicles passing a given cross section of road per hour and average speed of vehicles on Kennedy Road in a day

List of Figures

Figure 1. Location of the landslide studied in this paper (© Google Maps 2019)

Figure 2. Typical cross section of the slope studied in this paper

Figure 3. Plan view of the slope studied in this paper

Figure 4. Histogram and fitted PDF of yearly maximum i_{24} in Hong Kong

Figure 5. CDF of yearly maximum i_{24} in Hong Kong

Figure 6. PDF of travel distance of the landslide studied in this paper

Figure 7. Mean rates of different types of vehicles during different periods: (a) morning peak (b) normal period (c) evening peak. (1. Private buses, 2. Non-franchised public buses, 3. Franchised buses, 4. Taxis, 5. Private cars, 6. Public light buses, 7. Private light buses, 8. Goods vehicles, 9. Special purpose vehicles, 10. Government vehicles, 11. Motor cycles)

Figure 8. Probability distribution of number of private cars hit by the landslide studied in this paper during different periods for the case of $\alpha_j(\mathbf{S} = \mathbf{S}_i) = 1$: (a) morning peak (b) normal period (c) evening peak (d) considering uncertainty of failure time

Figure 9. Annual risk of elements hit by the landslide studied in this paper: (a) vehicles (b) persons. (1. Private buses, 2. Non-franchised public buses, 3. Franchised buses, 4. Taxis, 5. Private cars, 6. Public light buses, 7. Private light buses, 8. Goods vehicles, 9. Special purpose vehicles, 10. Government vehicles, 11. Motor cycles, 12. All types of vehicles)

Figure 10. Impact of failure probability of the slope on the landslide risk

Figure 11. Impact of distance between the landslide and the road on the landslide risk

Figure 12. Impact of density of vehicles on the landslide risk

https://doi.org/10.5194/nhess-2020-11
Preprint. Discussion started: 3 February 2020

Table 1. Percent, length and passenger capacity of vehicles in Hong Kong

Vehicles types	Percent (%)	Length (m)	Passenger capacity (persons)
Private buses	0.08	10	55
Non-franchised public buses	0.82	10	55
Franchised buses	0.72	10	55
Taxis	2.30	5	5
Private cars	71.41	5	5
Public light buses	0.50	9	33
Private light buses	0.39	9	33
Goods vehicles	13.77	12	2
Special purpose vehicles	0.23	5	1
Government vehicles	0.74	5	5
Motor cycles	9.24	2	1

https://doi.org/10.5194/nhess-2020-11
Preprint. Discussion started: 3 February 2020

Table 2. Number of vehicles passing a given cross section of road per hour and average speed of vehicles on Kennedy Road in a day

Periods in a day	Morning peak (7–9 am)	Normal period	Evening peak (5–7 pm)
q (vehicles per hour)	3000	1500	2800
v (km per hour)	15	30	15

https://doi.org/10.5194/nhess-2020-11
Preprint. Discussion started: 3 February 2020

Figure 1. Location of the landslide studied in this paper (© Google Maps 2019)

https://doi.org/10.5194/nhess-2020-11
Preprint. Discussion started: 3 February 2020

Natural Hazards and Earth System Sciences
Open Access
EGU
Discussions

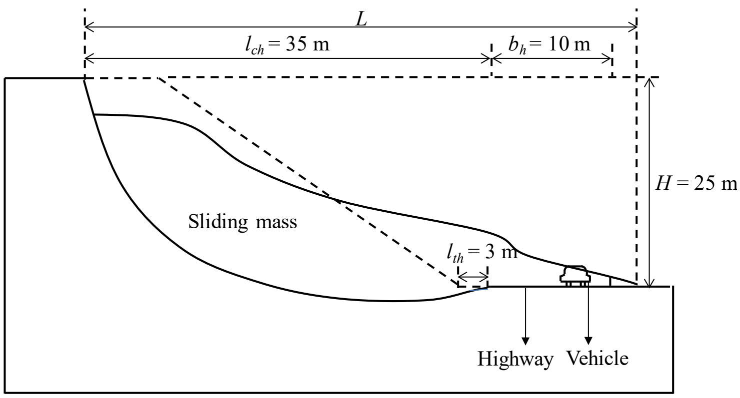

Figure 2. Typical cross section of the slope studied in this paper

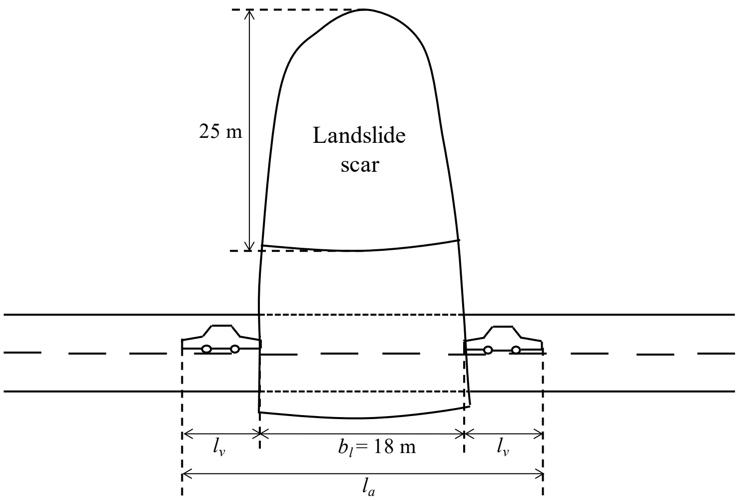

Figure 3. Plan view of the slope studied in this paper

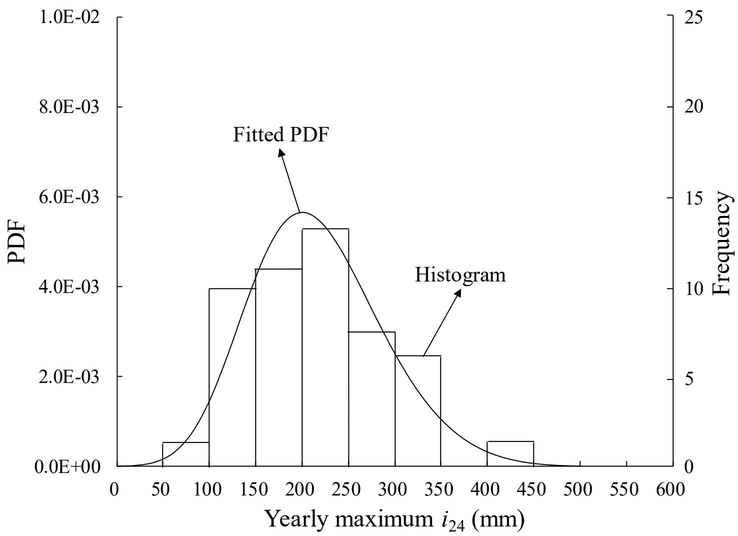

Figure 4. Histogram and fitted PDF of yearly maximum i_{24} in Hong Kong

https://doi.org/10.5194/nhess-2020-11
Preprint. Discussion started: 3 February 2020

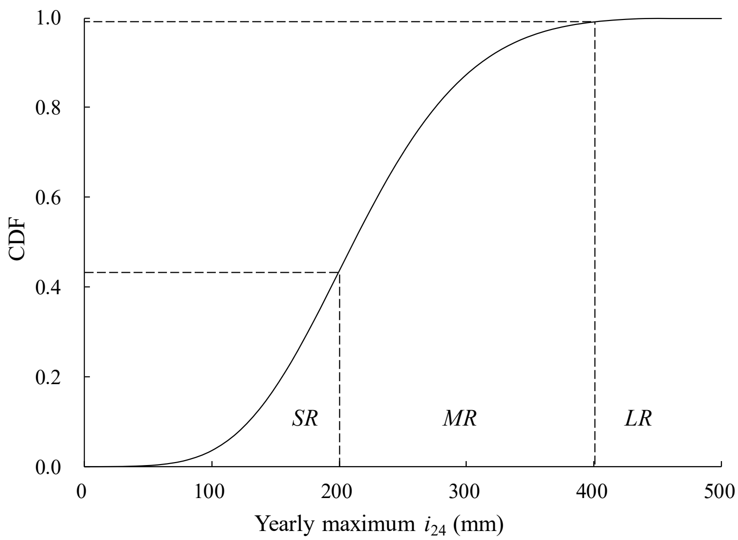

Figure 5. CDF of yearly maximum i_{24} in Hong Kong

https://doi.org/10.5194/nhess-2020-11
Preprint. Discussion started: 3 February 2020

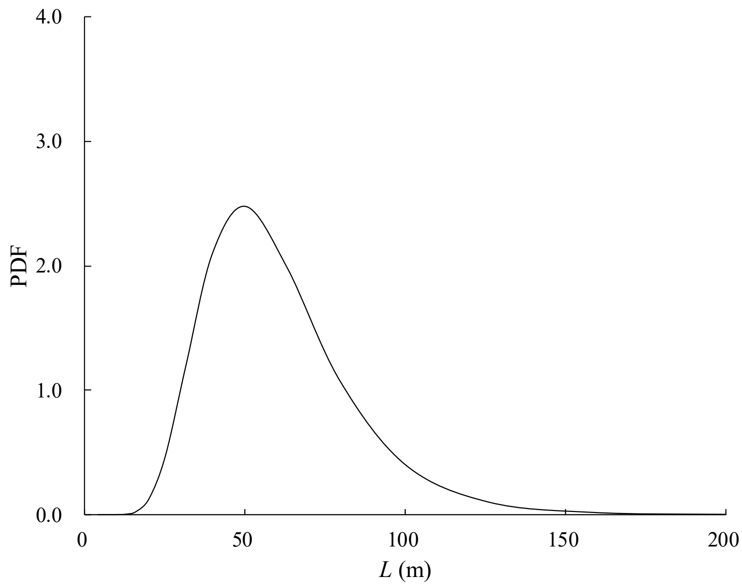

Figure 6. PDF of travel distance of the landslide studied in this paper

https://doi.org/10.5194/nhess-2020-11
Preprint. Discussion started: 3 February 2020

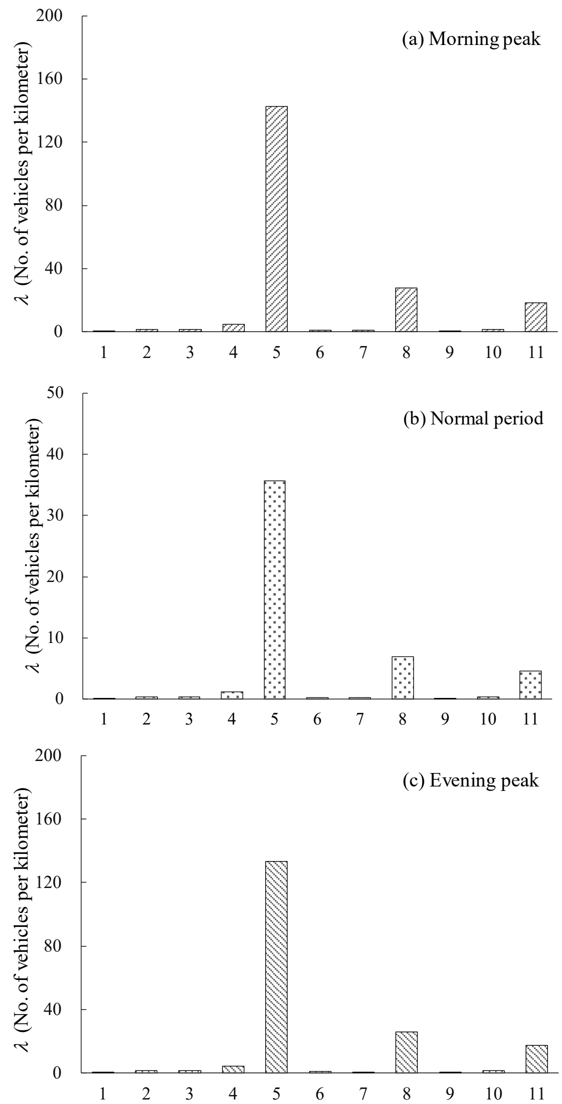

Figure 7. Mean rates of different types of vehicles during different periods: (a) morning peak (b) normal period (c) evening peak. (1. Private buses, 2. Non-franchised public buses, 3. Franchised buses, 4. Taxis, 5. Private cars, 6. Public light buses, 7. Private light buses, 8. Goods vehicles, 9. Special purpose vehicles, 10. Government vehicles, 11. Motor cycles)

https://doi.org/10.5194/nhess-2020-11
Preprint. Discussion started: 3 February 2020

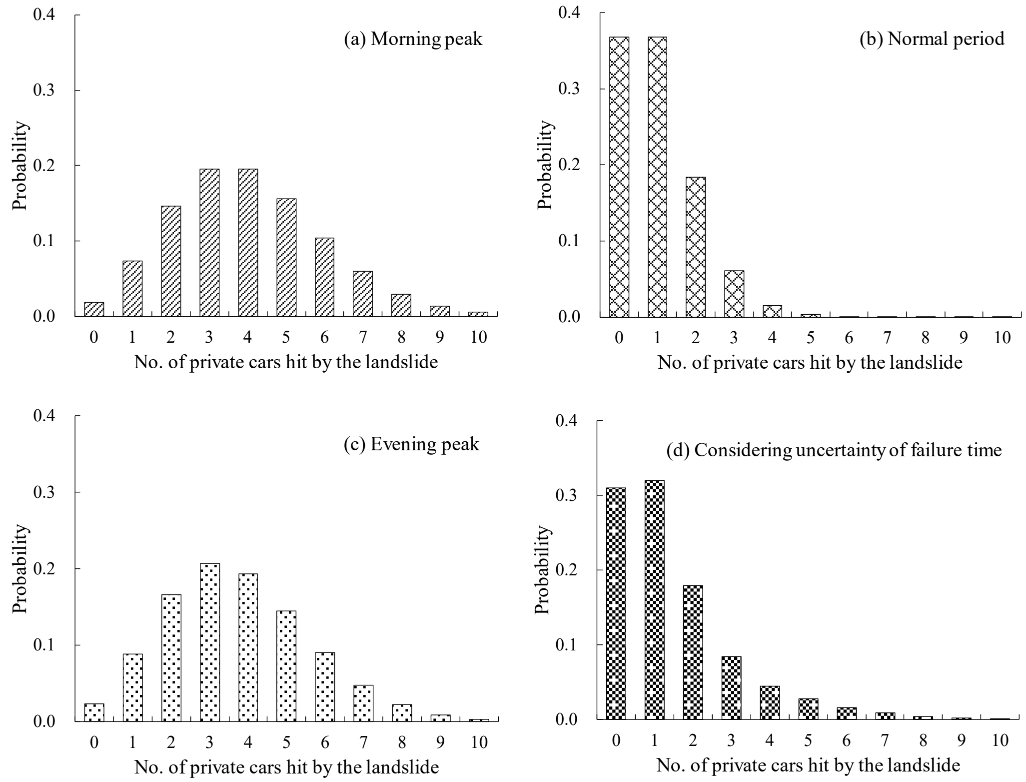

Figure 8. Probability distribution of number of private cars hit by the landslide studied in this paper during different periods for the case of $\alpha_j(\mathbf{S} = \mathbf{S}_i) = 1$: (a) morning peak (b) normal period (c) evening peak (d) considering uncertainty of failure time

https://doi.org/10.5194/nhess-2020-11
Preprint. Discussion started: 3 February 2020

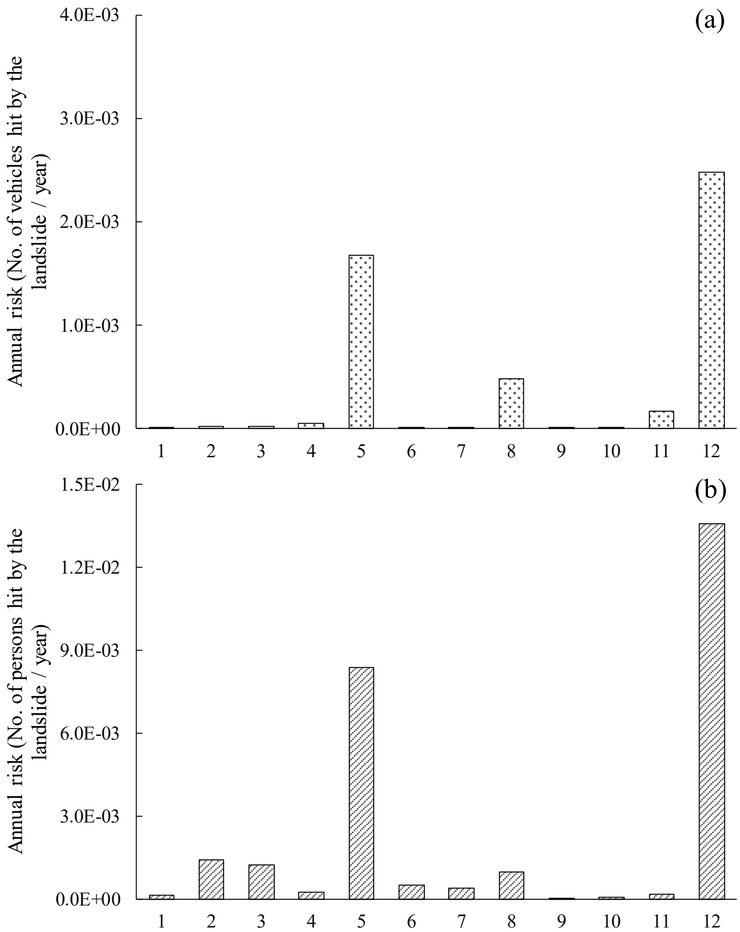

Figure 9. Annual risk of elements hit by the landslide studied in this paper: (a) vehicles (b) persons. (1. Private buses, 2. Non-franchised public buses, 3. Franchised buses, 4. Taxis, 5. Private cars, 6. Public light buses, 7. Private light buses, 8. Goods vehicles, 9. Special purpose vehicles, 10. Government vehicles, 11. Motor cycles, 12. All types of vehicles)

https://doi.org/10.5194/nhess-2020-11
Preprint. Discussion started: 3 February 2020

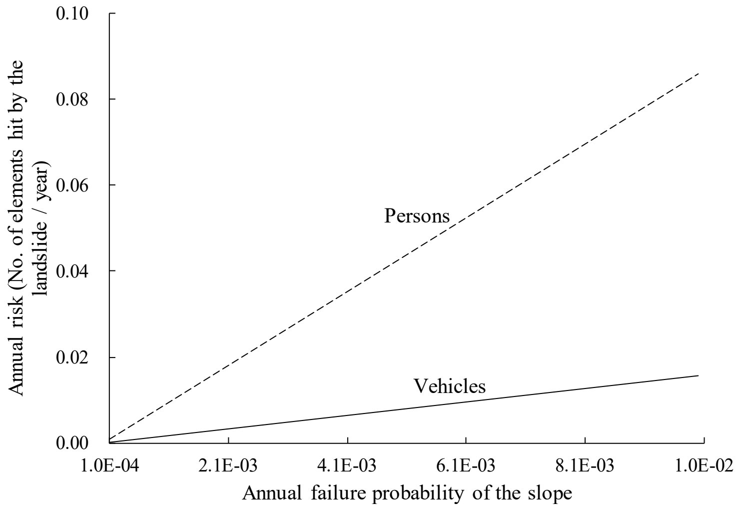

Figure 10. Impact of failure probability of the slope on the landslide risk

https://doi.org/10.5194/nhess-2020-11
Preprint. Discussion started: 3 February 2020

Natural Hazards and Earth System Sciences
Discussions

494 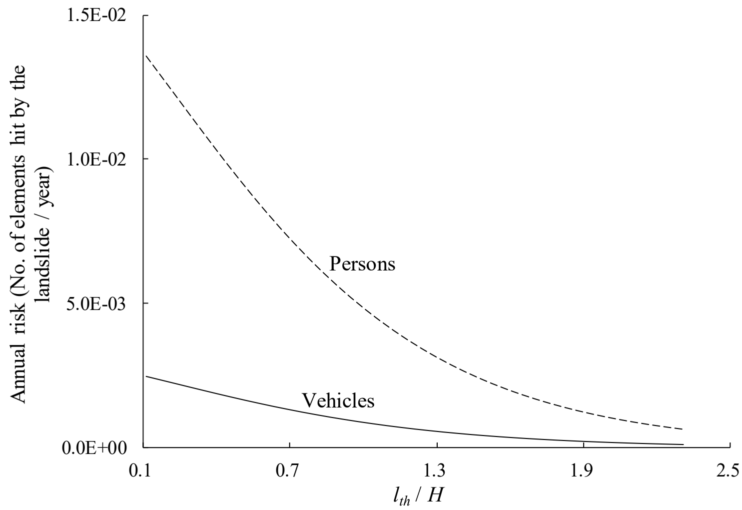

495

496 Figure 11. Impact of distance between the landslide and the road on the landslide risk

497

https://doi.org/10.5194/nhess-2020-11
Preprint. Discussion started: 3 February 2020

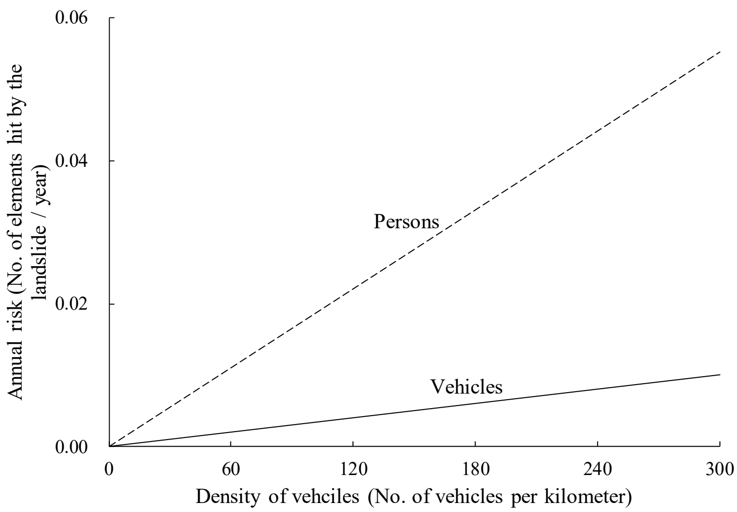

Figure 12. Impact of density of vehicles on the landslide risk